Journal of Sound and Vibration (2001) **242**(4), 559–575
doi:10.1006/jsvi.2000.3377, available online at http://www.idealibrary.com on IDEAL®

SIMULATION OF MOTION OF AN ELECTROMAGNETICALLY LEVITATED SPHERE

B. O. Ciocirlan, D. G. Beale and R. A. Overfelt

Department of Mechanical Engineering, Auburn University, AL 36849, *U.S.A.*

(*Received* 12 *October* 1998, *and in final form* 14 *August* 2000)

This paper studies the vibrator vertical motion of a metallic sphere placed in a time-varying magnetic field. The magnetic field is produced by a set of coaxial loops carrying high-frequency electric currents. A mathematical model for the motion of the sphere is developed and examined via numerical simulations for various materials and magnetic field parameters. The contribution of this paper is the development of the levitation force as a function of the specimen velocity.

1. INTRODUCTION

The process of electromagnetic levitation (EML) is now a well-known metallurgical technique to produce pure homogeneous melts. The procedure consists of placing a piece of metal in a time-varying magnetic field produced by a coil carrying a high-frequency electric current. The magnetic field induces eddy currents in the metal which lead to two major effects. On one hand, the interaction between the eddy currents and the applied magnetic field generates a Lorentz force that can support the specimen against gravity for appropriate values of the system parameters. On the other hand, the eddy currents heat or melt the specimen by Joule effect. This technique prevents the metal from contamination with impurities due to the container wall which is used in classical melting methods.

A difficulty encountered during the EML experiments is the stability of the suspended droplet inside the excitation coil. The stability problem has been discussed since the earliest works on electromagnetic levitation melting [1]. Static stability was formulated in terms of the optimal coil geometry, current intensity and frequency and Lorentz force acting on the specimen. Several analytical models to compute the Lorentz force were developed. All these models considered the levitation coil as a stack of current loops or helices.

Brisley and Thornton [2] performed an analysis of the electromagnetic levitation of a conductive sphere in an axially symmetric field produced by circular current loops. Formulas for the magnetic field both inside and outside of a sphere were developed. The levitation force was derived by considering the force on the loops due to the field of the induced eddy currents.

In deriving the experience for the Lorentz force, Rony [3] considered the specimen as a magnetic dipole interacting with a homogeneous magnetic field which varies slightly over the region of the dipole.

Lohöfer [4] re-examined Rony's assumptions and reported a solution based on solving the exact Maxwell's equations. The equations were solved analytically for a non-ferromagnetic conducting sphere placed arbitrarily in a sinusoidally alternating magnetic field.

0022-460X/01/190559 + 17 $35.00/0

Cummings and Blackburn [5] observed that the first mode of oscillation of a levitated specimen corresponds to the translational motion of the specimen, whereas the other modes are related to its surface oscillation. For certain values of the levitation system parameters, the vibratory motion of the specimen could be unstable. Mestel [6] suggested that one way to reduce the instabilities is to design the coil such that the specimen is stable with respect to small horizontal and vertical displacements.

The dynamic stability problem was also addressed. For dynamic stability analysis, the equations of motion of levitated specimens were first developed and then linearized about the operating point. Studying the linearized equation of motion, one can obtain useful information in terms of the damping and the stiffness of the specimen–coil system. Also, stability criteria can be derived. To investigate the stability of levitated specimens, Bocian and Young [7] developed a circuit model for a levitation system to form the linearized equation for the vertical motion of specimens. Two types of instabilities that often occur in practice were considered, namely, the growing vertical oscillation, leading to the ejection of the specimen through the supporting coil and the rupture of the suspended droplets. Regarding the former type, the system may become unstable when a capacitance is considered in the circuit of the levitation coil. If the capacitance is too small, the damping coefficient in the linearized equation of vertical motion of the specimen may become negative, leading to an unstable motion.

Holmes [8] proposed the linearized equations of horizontal and vertical motion for small specimens levitated in coils with axial symmetry. Stability criteria in terms of the natural frequencies of the system were also derived. The criteria are always satisfied for levitated non-magnetic specimens in regions of constant field gradient on the coil axis. No damping-related issue was addressed in this work.

Hence, to develop the equations of motion and to study the dynamic stability of levitated specimens, the availability of the expressions for the damping and stiffness forces is a prerequisite. Bocian [7] derived the levitation force as a function of the velocity of the specimen by using the circuit model of the specimen–coil system. Both damping and stiffness coefficients are available in the resulting linearized equation of motion. To obtain the expression for the levitation force, Holmes [8] first linearized the expression for the magnetic field intensity about an equilibrium position of the specimen along the coil axis. Then, the levitation force was derived by using the magnetic dipole model [9]. The resulting linearized equations of motion are in the form of free undamped vibration equation in which the stiffness coefficient must be positive for stable levitation. In this work, we propose an expression for Lorentz force due to the motion of the specimen with respect to the coil by considering the exact solutions of Maxwell's equations for the specimen–coil system. We used this expression for the Lorentz force to obtain non-linear and the linearized equation for the vertical motion of spherical specimens. Hence, the damping and stiffness of the specimen–coil system can be calculated in terms of the geometric and source parameters of the coil.

The mathematical model is developed in section 2. The results of the numerical simulations are discussed in section 3. Finally, several concluding remarks are made.

2. MATHEMATICAL MODEL

Let us consider the levitation system shown in Figure 1. It is composed of N coaxial circular loops of current lying in parallel planes (stack of loops). The radius of each loop is denoted by b_k, $k = 1, \ldots, N$. The loops carry an alternating electric current $\Re[I_k e^{j\omega t}]$, where I_k is the peak value, ω is the angular frequency ($\omega = 2\pi f$, where f is the frequency), t is the

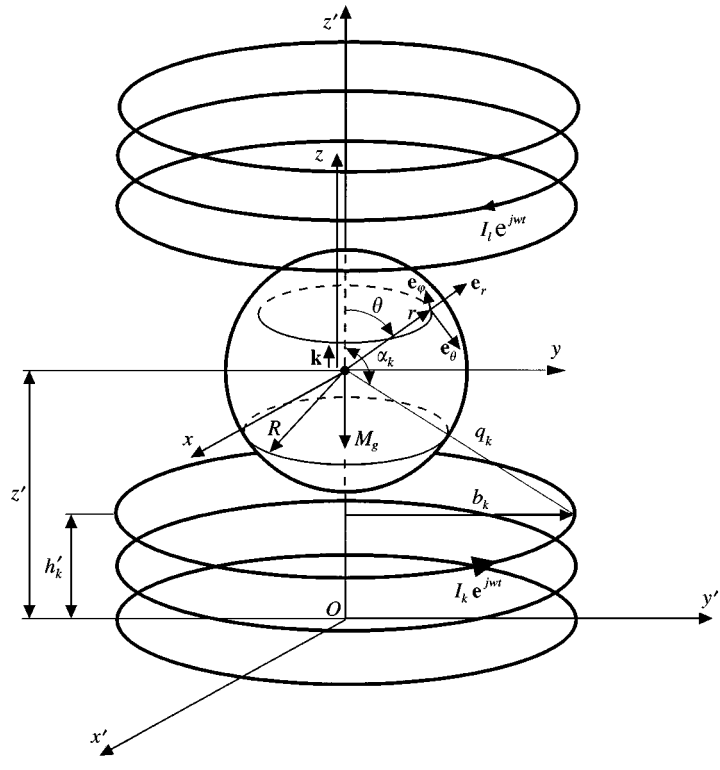

Figure 1. Levitation system.

time, $j = \sqrt{-1}$ and $\Re(\cdot)$ denotes the real part of the complex current. The current is positive for the lower loops and negative for upper loops. The body to be levitated is a conductive sphere of radius R, mass M, electric conductivity σ, and magnetic permeability μ_i and its center lies on the axis of symmetry of the system. The Cartesian reference frame (x', y', z') is fixed at the center of the bottom loop and the unit vector of the z'-axis is denoted by $\mathbf{k}'$. The Cartesian and spherical reference frames, (x, y, z) and (r, θ, φ) respectively, are attached to the conductive sphere in motion and their origins are at the center of the sphere. In this presentation, z is constrained to be parallel to z' and the sphere does not spin. The unit vector of z-axis of the Cartesian reference frame (x, y, z) is denoted by $\mathbf{k}$ and the unit vectors of the spherical reference frame (r, θ, φ) by $\mathbf{e}_r$, $\mathbf{e}_\theta$, $\mathbf{e}_\varphi$ respectively. The kth loop is defined by $(r = q_k, \theta = \alpha_k)$, with respect to the spherical reference frame. The conductive sphere moves along z'-axis with velocity $\mathbf{v}'$. Its center has the co-ordinate $z' = z'(t)$ with respect to the fixed Cartesian reference frame (x', y', z'). No motion parallel to the plane of the loops is considered in this model.

The time-averaged Lorentz force density exerted on the sphere is given by

$$\mathbf{f} = \tfrac{1}{2}\Re(\underline{\mathbf{J}} \times \underline{\mathbf{B}}^*), \tag{1}$$

where $\underline{\mathbf{J}}$ is the induced eddy current density, $\underline{\mathbf{B}}$ is the magnetic flux density, underscore denotes a complex variable and $\Re(\cdot)$ and $*$ are the real part and the complex conjugate of a complex variable respectively. In the above equation, the magnetic field quantities are measured with respect to the unprimed reference frame which is attached to the body in motion. From now on, the unprimed symbols denote quantities measured in the moving

reference frame, while the primed symbols denote quantities measured in the fixed reference frame.

The time-averaged Lorentz force density in equation (1) can be expressed with respect to the fixed reference frame by considering the following set of transformations [10]:

$$\mathbf{J} = \mathbf{J}', \qquad \mathbf{B} = \mathbf{B}', \qquad \mathbf{E} = \mathbf{E}' + \mathbf{v}' \times \mathbf{B}', \tag{2–4}$$

where $\mathbf{E}$ and $\mathbf{E}'$ are the electric field intensity measured in the mobile and fixed reference frames respectively. Applying Ohm's law, which states that

$$\mathbf{J} = \sigma \mathbf{E}, \tag{5}$$

along with equations (2)–(4), and considering the fact that the force is independent of the reference frame in which it is measured, that is, $\mathbf{f} = \mathbf{f}'$, the time-averaged Lorentz force density in equation (1) reads

$$\mathbf{f}' = \tfrac{1}{2}\Re[\sigma(\underline{\mathbf{E}}' \times \underline{\mathbf{B}}'^{*}) + \sigma(\mathbf{v}' \times \mathbf{B}') \times \underline{\mathbf{B}}'^{*}] = \mathbf{f}'_s + \mathbf{f}'_d. \tag{6}$$

We called the first part of the time-averaged Lorentz force density in equation (6),

$$\mathbf{f}'_s = \tfrac{1}{2}\Re[\sigma(\underline{\mathbf{E}}' \times \underline{\mathbf{B}}'^{*})],$$

the stiffness component, and the second part,

$$\mathbf{f}'_d = \tfrac{1}{2}\Re[\sigma(\mathbf{v}' \times \underline{\mathbf{B}}') \times \underline{\mathbf{B}}'^{*}],$$

the damping component.

In developing the expression for $\mathbf{f}'_s$, the effects of the motion were neglected. The magnetic field quantities can be computed with respect to either fixed or mobile reference frames. For convenience, the spherical reference frame (r, θ, φ) was chosen to develop the expression for $\mathbf{f}_s$. Therefore, the stiffness component of the time-averaged Lorentz force density reads

$$\mathbf{f}_s = \tfrac{1}{2}\Re[(-\mathrm{j}\omega\sigma \underline{\mathbf{A}}_\varphi) \times \underline{\mathbf{B}}^{*}], \tag{7}$$

where $\underline{\mathbf{A}}_\varphi$ and $\underline{\mathbf{B}}$ are the magnetic vector potential and the magnetic flux density in the sphere, respectively, as they were reported by Brisley and Thornton [2].

The damping component $\mathbf{f}_d$ was obtained by neglecting the diffusion of the magnetic field into the spherical conductor during the motion. Therefore, the damping component is given by

$$\mathbf{f}'_d = \tfrac{1}{2}\Re[\sigma(\mathbf{v}' \times \underline{\mathbf{B}}'_{app}) \times \underline{\mathbf{B}}'^{*}_{app}], \tag{8}$$

where $\underline{\mathbf{B}}'_{app}$ is the applied magnetic flux density. The expressions for the magnetic field produced by a single loop computed in a spherical reference frame with the origin placed on the axis perpendicular to the plane of the loop at its center are available in the book by Smythe [9]. These expressions, when they are written with respect to the spherical reference frame (r, θ, φ) defined in Figure 1, read, respectively,

$$B_{app,r} = -\frac{\mu_i}{2} \sum_{k=1}^{N} \frac{I_k \sin\alpha_k}{q_k} \sum_{n=1}^{\infty} P_n^1(\cos\alpha_k) P_n(\cos\theta) \left(\frac{r}{q_k}\right)^{n-1}, \tag{9}$$

$$B_{app,\theta} = -\frac{\mu_i}{2} \sum_{k=1}^{N} \frac{I_k \sin\alpha_k}{q_k} \sum_{n=1}^{\infty} \frac{1}{n} P_n^1(\cos\alpha_k) P_n(\cos\theta) \left(\frac{r}{q_k}\right)^{n-1}, \tag{10}$$

$$B_{app,\varphi} = 0, \tag{11}$$

where $P_n(\cdot)$ is the Legendre polynomial of degree n and $P_n^1(\cdot)$ the associate Legendre polynomial of degree n and order 1. To use the expressions for the applied magnetic field in equations (9) and (10), the damping component of the time-averaged Lorentz force density has to be computed with respect to the spherical reference frame (r, θ, φ). Therefore, the damping component has the form

$$\mathbf{f}_d = \tfrac{1}{2}\Re[\sigma(-\mathbf{v}\times\underline{\mathbf{B}}_{app})\times\underline{\mathbf{B}}^*_{app}], \tag{12}$$

where $\mathbf{v}$ is the velocity of the magnetic field as if the conducting sphere is fixed and the magnetic field moves along the z-axis with a velocity equal to $\mathbf{v}'$, but in the opposite direction.

The time-averaged Lorentz force density $\mathbf{f}$ measured with respect to the mobile spherical reference frame was obtained by summing equations (7) and (12), result in

$$\mathbf{f} = \mathbf{f}_s + \mathbf{f}_d = \tfrac{1}{2}\Re[(-\mathrm{j}\omega\sigma\underline{\mathbf{A}}_{\varphi})\times\underline{\mathbf{B}}^*] - \tfrac{1}{2}\Re[\sigma(\mathbf{v}\times\underline{\mathbf{B}}_{app})\times\underline{\mathbf{B}}^*_{app}]. \tag{13}$$

Then, the levitation force which supports the sphere against gravity was found by integrating $\mathbf{f}$ in equation (13) over the volume of the sphere. With respect to the reference frames shown in Figure 1, the volume integral to be sought is of the form

$$\begin{aligned} F_z &= \int_{Sphere} \mathbf{f}\cdot\mathbf{k}\,\mathrm{d}(Vol) \\ &= \int_{Sphere} \mathbf{f}_s\cdot\mathbf{k}\,\mathrm{d}(Vol) + \int_{Sphere} \mathbf{f}_d\cdot\mathbf{k}\,\mathrm{d}(Vol) \\ &= F_{z,s} + F_{z,d}, \end{aligned} \tag{14}$$

where

$$F_{z,s} = \int_{Sphere} \mathbf{f}_s\cdot\mathbf{k}\,\mathrm{d}(Vol) \tag{15}$$

is the stiffness component and

$$F_{z,d} = \int_{Sphere} \mathbf{f}_d\cdot\mathbf{k}\,\mathrm{d}(Vol) \tag{16}$$

is the damping component of the Lorentz force.

In the next two subsections, the expressions for damping and stiffness components of the levitation force were considered.

2.1. THE DAMPING COMPONENT $F_{z,d}$

Expanding the vectorial product in equation (12), with $\mathbf{v} = u\mathbf{k} = v(\cos\theta\,\mathbf{e}_r - \sin\theta\,\mathbf{e}_\theta)$, gives

$$\begin{aligned} \mathbf{f}_d = \tfrac{1}{2}\Re[&\sigma v(B^2_{app,\theta}\cos\theta + B_{app,\theta}B_{app,r}\sin\theta)\mathbf{e}_r \\ &- \sigma v(B_{app,r}B_{app,\theta}\cos\theta + B^2_{app,r}\sin\theta)\mathbf{e}_\theta] \end{aligned}$$

$$= \tfrac{1}{2}\sigma v(B_{app,\theta}^2 \cos\theta + B_{app,\theta} B_{app,r} \sin\theta)\mathbf{e}_r$$

$$- \tfrac{1}{2}\sigma v(B_{app,r} B_{app,\theta} \cos\theta + B_{app,r}^2 \sin\theta)\mathbf{e}_\theta. \tag{17}$$

Substituting equation (17) into equation (16) and rearranging the terms, the damping component of the Lorentz force reads

$$F_{z,d} = \int_{Sphere} \mathbf{f}_d \cdot \mathbf{k}_s \, \mathrm{d}(Vol)$$

$$= v\pi\sigma \int_0^R \int_{-1}^1 (B_{app,\theta} \cos\theta + B_{app,r} \sin\theta)^2 r^2 \, \mathrm{d}r \, \mathrm{d}(\cos\theta). \tag{18}$$

Substituting equations (9) and (10), which provide the expressions for $B_{app,r}$ and $B_{app,\theta}$, respectively, into equation (18), the damping component can be written as

$$F_{z,d} = v \frac{\pi\sigma\mu_i^2}{4} \sum_{l=1}^{N} \frac{I_l \sin\alpha_l}{q_l} \sum_{k=1}^{N} \frac{I_k \sin\alpha_k}{q_k} \sum_{m=1}^{\infty} \sum_{n=1}^{\infty} \frac{P_m^1(\cos\alpha_l) P_n^1(\cos\alpha_k)}{q_l^{m-1} q_k^{n-1}}$$

$$\times \int_0^R r^{m+n} \, \mathrm{d}r \int_{-1}^1 \left[\sin\theta P_m(\cos\theta) + \frac{\cos\theta}{m} P_m^1(\cos\theta) \right]$$

$$\times \left[\sin\theta P_n(\cos\theta) + \frac{\cos\theta}{\mathrm{n}} P_n^1(\cos\theta) \right] \mathrm{d}(\cos\theta). \tag{19}$$

The expression for $F_{z,d}$ in equation (19) can be further simplified. Solving the integral with respect to r, which simply gives

$$\int_0^R r^{m+n} \, \mathrm{d}r = \frac{R^{m+n+1}}{m+n+1}, \tag{20}$$

expanding the product in the second integral in equation (19), using the following relationships for Legendre polynomials:

$$x P_n^1(x) = \frac{1}{2n+1} [n P_{n+1}^1(x) + (n+1) P_{n-1}^1(x)] \tag{21}$$

and

$$\sqrt{1-x^2} \, P_n^1(x) = \frac{n(n+1)}{2n+1} [P_{n+1}(x) - P_{n-1}(x)], \tag{22}$$

and the orthogonality of the Legendre polynomials,

$$\int_{-1}^1 P_m^l(x) P_n^l(x) \, \mathrm{d}x = \begin{cases} 0, & m \neq n, \\ \dfrac{2}{2n+1} \dfrac{(n+l)!}{(n-l)!}, & m = n, \end{cases} \tag{23}$$

re-indexing and rearranging, the double summation in m and n in equation (19) was transformed into a single one as shown in the final expression for the damping component,

$$F_{z,d} = v\frac{\pi\sigma\mu_i^2 R}{2}\sum_{l=1}^{N} I_l \sin\alpha_l \sum_{k=1}^{N} I_k \sin\alpha_k \sum_{n=2}^{\infty}\frac{n-1}{n(4n^2-1)}$$

$$\times\left(\frac{R}{q_l}\right)^n\left(\frac{R}{q_k}\right)^n P_n^1(\cos\alpha_l)P_n^1(\cos\alpha_k). \tag{24}$$

2.2. THE STIFFNESS COMPONENT $F_{z,s}$

To develop the expression for $F_{z,s}$, the procedure was straightforward. First, the expression for $\mathbf{f}_s$ given by the first term in equation (13) was obtained and, then, the dot product and the integration over the volume of the sphere in equation (15) were performed. The expressions for $\underline{\mathbf{A}}_\varphi$ and $\underline{\mathbf{B}}$ in equation (13) developed in the paper by Brisley and Thornton [2] were considered. Since the procedure applied in this work to obtain the expression for $F_{z,s}$ is similar to that reported in Li [11] for the case of a single loop, only the final form of the expression for $F_{z,s}$ is given, namely,

$$F_{z,s} = -\frac{\pi\omega\sigma\mu_i^2 R}{4}\sum_{l=1}^{N}\mathrm{I}_l\sin\alpha_l\sum_{k=1}^{N}\mathrm{I}_k\sin\alpha_k\sum_{n=1}^{\infty}\frac{1}{n+1}\left(\frac{R}{q_l}\right)^{n+1}\left(\frac{R}{q_k}\right)^{n+1}$$

$$\times[q_k P_{n+1}^1(\cos\alpha_l)P_n^1(\cos\alpha_k)\mathscr{M}_{n+1,n} + q_l P_n^1(\cos\alpha_l)P_{n+1}^1(\cos\alpha_k)\mathscr{N}_{n,n+1}], \tag{25}$$

where

$$\mathscr{M}_{n+1,n} = \Re\left[\frac{1}{\underline{\mathscr{H}}_{n+1,n}}\left(\mathrm{I}_{n-1/2}(\underline{\gamma}^*R)\mathrm{I}_{n-3/2}(\underline{\gamma}R) - \frac{2(2n+1)}{R}\,\mathrm{IB1}\right)\right]$$

$$+\,\Im\left[\frac{1}{\underline{\mathscr{H}}_{n+1,n}}\left(-\mathrm{I}_{n-1/2}(\underline{\gamma}R)\mathrm{I}_{n-3/2}(\underline{\gamma}^*R) + \frac{2(2n+1)}{R}\,\mathrm{IB2}\right)\right] \tag{26}$$

and

$$\mathscr{N}_{n,n+1} = \Re\left[\frac{\mathrm{I}_{n+1/2}(\underline{\gamma}^*R)\mathrm{I}_{n-1/2}(\underline{\gamma}R)}{\underline{\mathscr{H}}_{n,n+1}}\right] - \Im\left[\frac{\mathrm{I}_{n+1/2}(\underline{\gamma}R)\mathrm{I}_{n-1/2}(\underline{\gamma}^*R)}{\underline{\mathscr{H}}_{n,n+1}}\right]. \tag{27}$$

In equations (26) and (27), $\Re(\cdot)$ and $\Im(\cdot)$ denote the real and imaginary parts of a complex variable, respectively, $\mathrm{I}_{n\pm1/2}(\cdot)$ and $\mathrm{I}_{n\pm3/2}(\cdot)$ are the modified Bessel function of the first kind of complex argument $\underline{\gamma}R$ (or $\underline{\gamma}^*R$), $\underline{\gamma} = \sqrt{j\omega\sigma\mu_i}$ and $\underline{\mathscr{H}}$, IB1 and IB2 are given by the following expressions, respectively:

$$\underline{\mathscr{H}}_{m,n} = \left[\underline{\gamma}R\mathrm{I}_{m-1/2}(\underline{\gamma}R) + \left(\frac{\mu_i}{\mu_o}-1\right)m\mathrm{I}_{m+1/2}(\underline{\gamma}R)\right]$$

$$\times\left[\underline{\gamma}^*R\mathrm{I}_{n-1/2}(\underline{\gamma}^*R) + \left(\frac{\mu_i}{\mu_o}-1\right)n\mathrm{I}_{n+1/2}(\underline{\gamma}^*R)\right],$$

$$\mathrm{IB1} = \int_0^R \mathrm{I}_{n+1/2}(\underline{\gamma} r)\mathrm{I}_{n-1/2}(\underline{\gamma}^* r)\,\mathrm{d}r = \sum_{p=0}^{\infty}\sum_{s=0}^{\infty}\frac{1}{p!}\frac{1}{\Gamma(n+p+3/2)}$$
$$\times\frac{1}{s!}\frac{1}{\Gamma(n+s+1/2)}\left(\frac{\underline{\gamma}}{2}\right)^{n+2p+1/2}\left(\frac{\underline{\gamma}^*}{2}\right)^{n+2s-1/2}\frac{R^{2(n+p+s)+1}}{2(n+p+s)+1} \quad (28)$$

and

$$\mathrm{IB2} = \int_0^R \mathrm{I}_{n+3/2}(\underline{\gamma} r)\mathrm{I}_{n+1/2}(\underline{\gamma}^* r)\,\mathrm{d}r = \sum_{p=0}^{\infty}\sum_{s=0}^{\infty}\frac{1}{p!}\frac{1}{\Gamma(n+p+5/2)}$$
$$\times\frac{1}{s!}\frac{1}{\Gamma(n+s+3/2)}\left(\frac{\underline{\gamma}}{2}\right)^{n+2p+3/2}\left(\frac{\underline{\gamma}^*}{2}\right)^{n+2s+1/2}\frac{R^{2(n+p+s)+3}}{2(n+p+s)+3}. \quad (29)$$

In equations (28) and (29), the following series expansion for the modified Bessel functions of the first kind was considered:

$$\mathrm{I}_\nu(\underline{x}) = \sum_{p=0}^{\infty}\frac{1}{p!}\frac{1}{\Gamma(\nu+p+1)}\left(\frac{\underline{x}}{2}\right)^{\nu+2p}, \quad (30)$$

where $\Gamma(\cdot)$ is the Gamma function of a complex argument $\underline{x}$.

2.3. EQUATION OF MOTION

The equation of vertical motion of the conductive sphere was derived by applying Newton' second law, that is,

$$M\frac{\mathrm{d}^2 z'}{\mathrm{d}t^2} = F_{z'} - Mg, \quad (31)$$

where $\mathrm{d}^2z'/\mathrm{d}t^2$ is the acceleration of the sphere, $F_{z'}$ Lorentz force measured with respect to the primed reference frame, and g the gravitational acceleration. The levitation force in equation (31) is measured with respect to the fixed reference frame and, consequently, the stiffness and damping components of the levitation force need also to be expressed in that reference frame. In their expressions, the quantities which depend upon the vertical co-ordinate z are the sine and cosine functions,

$$\sin\alpha_k = \frac{b_k}{q_k}, \qquad \cos\alpha_k = -\frac{z_1 - (h_k - h_1)}{q_k}, \quad (32, 33)$$

$$q_k = \sqrt{b_k^2 + [z_1 - (h_k - h_1)]^2}, \quad (34)$$

where z_1 is the distance from the origin of the unprimed reference frame to the plane of the bottom loop. Therefore, to express the forces with respect to the fixed reference frame, the transformation

$$z_1 = |z(t)| = z'(t) - h_1 \quad (35)$$

was applied in equations (32)–(34). The velocity of the moving sphere has to be computed in the fixed reference frame too. The relationship between the velocities measured in the

mobile and fixed reference frames,

$$\mathbf{v} = -\mathbf{v}', \tag{36}$$

was also considered.

Upon substituting equations (32)–(36) into equations (25) and (24), writing the velocity of the spheres as $v' = \mathrm{d}z'/\mathrm{d}t$, and manipulating, the equation of vertical motion reads

$$\frac{\mathrm{d}^2 z'}{\mathrm{d}t^2} + \frac{C(z')}{M}\frac{\mathrm{d}z'}{\mathrm{d}t} + \frac{K(z')}{M} + g = 0, \tag{37}$$

where $C(z')$ and $K(z')$ are given by the expressions

$$C(z') = -\frac{1}{v'}F_{z',d} = \frac{\pi\sigma\mu_i^2 R}{2}\sum_{l=1}^{N}\mathrm{I}_l \sin\alpha_l' \sum_{k=1}^{N}\mathrm{I}_k \sin\alpha_k' \sum_{n=2}^{\infty}\frac{n-1}{n(4n^2-1)}\left(\frac{R}{q_l'}\right)^n\left(\frac{R}{q_k'}\right)^n$$
$$\times P_n^1(\cos\alpha_l')P_n^1(\cos\alpha_k') \tag{38}$$

and

$$K(z') = -F_{z',s}$$
$$= \frac{\pi\omega\sigma\mu_i^2 R}{4}\sum_{l=1}^{N}\mathrm{I}_l \sin\alpha_l' \sum_{k=1}^{N}\mathrm{I}_k \sin\alpha_k' \sum_{n=1}^{\infty}\frac{1}{n+1}\left(\frac{R}{q_l'}\right)^{n+1}\left(\frac{R}{q_k'}\right)^{n+1}$$
$$\times [q_k' P_{n+1}^1(\cos\alpha_l')P_n^1(\cos\alpha_k')\mathscr{M}_{n+1,n} + q_l' P_n^1(\cos\alpha_l')P_{n+1}^1(\cos\alpha_k')\mathscr{N}_{n,n+1}], \tag{39}$$

where

$$\sin\alpha_k' = \frac{b_k'}{q_k'}, \qquad \cos\alpha_k' = -\frac{z'(t) - h_k'}{q_k'}, \tag{40, 41}$$

$$q_k' = \sqrt{b_k'^2 + [z'(t) - h_k']^2} \tag{42}$$

and $\mathscr{M}_{n+1,n}$ and $\mathscr{N}_{n,n+1}$ are given by equations (26) and (27) respectively.

2.4. LINEARIZATION OF THE EQUATION OF MOTION

Small perturbations from the equilibrium position of the levitated sphere can be predicted approximately by linearized equations of motion [10]. Assuming that $z'(t)$ has the form

$$z'(t) = z_e' + \zeta(t), \tag{43}$$

where z_e' is the equilibrium position and $\zeta(t)$ the small perturbation, the non-linear damping and stiffness coefficients $C(z')$ and $K(z')$ can be expanded in Taylor series about z_e', resulting

$$C(z') = C(z_e') + \frac{1}{1!}\frac{\mathrm{d}C(z')}{\mathrm{d}z'}\bigg|_{z'=z_e'}\zeta + \frac{1}{2!}\frac{\mathrm{d}^2 C(z')}{\mathrm{d}z'^2}\bigg|_{z'=z_e'}\zeta^2 + \cdots$$
$$= C_0 + C_1\zeta + C_2\zeta^2 + \cdots, \tag{44}$$

$$K(z') = K(z'_e) + \frac{1}{1!}\frac{\mathrm{d}K(z')}{\mathrm{d}z'}\bigg|_{z'=z'_e}\zeta + \frac{1}{2!}\frac{\mathrm{d}^2K(z')}{\mathrm{d}z'^2}\bigg|_{z'=z'_e}\zeta^2 + \cdots$$

$$= K_0 + K_1\zeta + K_2\zeta^2 + \cdots. \tag{45}$$

Retaining the first term in equation (44), the first two terms in equation (45), and observing that $K_0/M + g = 0$, the linearized equation of motion, which approximates equation (37), reads

$$\frac{\mathrm{d}^2\zeta}{\mathrm{d}t^2} + \frac{C_0}{M}\frac{\mathrm{d}\zeta}{\mathrm{d}t} + \frac{K_1}{M}\zeta = 0. \tag{46}$$

The expressions for C_0 and K_1 can be developed from equations (38) and (39), respectively, by computing $C_0 = C(z'_e)$ and $K_1 = \mathrm{d}K(z')/\mathrm{d}z'|_{z'=z'_e}$.

Comparing equation (46) with the equation for the viscously damped free vibration of the form [12]

$$\frac{\mathrm{d}^2\zeta}{\mathrm{d}t^2} + 2\xi\omega_n\frac{\mathrm{d}\zeta}{\mathrm{d}t} + \omega_n^2\zeta = 0 \tag{47}$$

and identifying the coefficients, the expressions for the damping factor ξ and natural frequency ω_n were obtained, respectively,

$$\xi = \frac{C_0}{2M\omega_n}, \qquad \omega_n = \sqrt{\frac{K_1}{M}}. \tag{48, 49}$$

Depending on the damping factor ξ, the following three situations can occur: underdamped motion ($\xi < 1{\cdot}0$), critically damped motion ($\xi = 1{\cdot}0$), and overdamped motion ($\xi > 1{\cdot}0$).

3. RESULTS AND DISCUSSION

Some comments regarding the mathematical model in section 2 should be made at this point.

The expression for the damping component $\mathbf{f}_d$ of the Lorentz force density in equation (12) was obtained by neglecting the diffusion of the magnetic field in the conductor during the motion. It was also assumed that the magnetic field induced by the sphere current $\sigma(\mathbf{v} \times \underline{\mathbf{B}}_{app})$ is negligible compared with the imposed field $\underline{B}_{app}$. Therefore, special attention must be paid to the selection of the conductive materials to which the mathematical model developed in section 2 can be applied. One way to decide whether the applied magnetic field $\underline{\mathbf{B}}_{app}$ is altered by the motion is to compute the dimensionless quantity called the magnetic Reynolds number. It can be defined by the relationship

$$R_m = \mu_i\sigma l v,$$

where $\mu_i = \mu_r\mu_0$ is the magnetic permeability, μ_r the relative magnetic permeability, μ_0 the magnetic permeability of free space, σ the electric conductivity, l a reference length, and v a reference velocity. If R_m is significant compared with unity, the applied magnetic field is altered appreciably by the motion. If R_m is small compared with unity, then the magnetic field induced by the current $\sigma(\mathbf{v} \times \underline{\mathbf{B}}_{app})$ can be neglected. The length l can be chosen as the same order as the radius R of the spherical specimens considered for numerical simulations,

that is, $l = R \approx 0{\cdot}001$ m. Let us discuss first the class of diamagnetic conductors, or. generally, the conductors with $\mu_i = \mu_0 = 4\pi \times 10^{-7}$ H/m and electric conductivity of the order 10^7 S/m. For this type of conductors, the magnetic Reynolds number is of the order $R_m \approx 0{\cdot}01v$. Typical values for the velocity measured during levitation experiments of such materials are in the range 0·1–1·0 m/s. Therefore, $R_m \approx 0{\cdot}001$–$0{\cdot}01$ and, in this case, the applied magnetic field $\underline{\mathbf{B}}_{app}$ is not altered by the motion. Now, let us consider linear ferromagnetic materials with $\mu_r \approx 100$–1000. The same values for the electric conductivity and velocity as in the previous case can be applied, resulting $R_m \approx 0{\cdot}1$–$10{\cdot}0$. It follows that the applied magnetic field $\underline{\mathbf{B}}_{app}$ is altered by the motion depending upon the properties of the particular material. For example, the magnetic Reynolds number computed for aluminum and copper, with the electromagnetic properties listed in Table 1 [13, 14] and $v = 1{\cdot}0$ m/s gives $R_m \approx 0{\cdot}05$ and $0{\cdot}08$ respectively. Therefore, the mathematical model proposed in this work is appropriate for aluminum and copper, and, in general, for all diamagnetic conductors. Instead, the magnetic Reynolds number gives $R_m \approx 4{\cdot}0$ for nickel, which is a ferromagnetic material. Since this value of R_m is comparable with the unity, special attention must be paid in interpreting the results of the theory for this class of materials.

Figure 2 shows the typical plots for stiffness and damping coefficients, $K(z')$ and $C(z')$, respectively, with respect to position z' of the sphere for a levitation system composed of two loops and an aluminum specimen. Similar plots can be obtained for copper specimens. As one can notice from Figure 2(b), the damping coefficient $C(z')$ given by equation (38) is positive for any position of the sphere. Therefore, the damping component of the levitation force $F_{z',d} = -v'C(z')$ and the velocity v' have opposite directions, which means that $F_{z',d}$ tends to retard the motion of the sphere. This result is entirely consistent with Lenz's rule, which states that the effect of the motion of a conductive body in a non-uniform magnetic field tends to cancel out the cause that producers it. For the levitation system studied here, the cause that initiates the motion is the stiffness component $F_{z',s}$, which pushes the specimen towards the equilibrium position. The effect is the damping component $F_{z',d}$, which opposes the action of the stiffness component, giving rise to a damped oscillation about the equilibrium position.

The linearization procedure in section 2.4 for equation (37) is also shown in Figure 2. The equilibrium position z'_e in equation (43) is given by the solution of the equation $K(z'_e) = Mg$. The expressions for $K(z')$ and $C(z')$ were expanded in Taylor series about the resulted equilibrium position, as described in section 2.4. Retaining the first two terms for $K(z')$ and the first term for $C(z')$, the plots of the linearized expressions versus z' are represented by the straight lines in Figures 2(a) and 2(b) respectively. For small perturbations about z'_e, the stiffness and damping coefficients can be approximated by the values of the coefficients K_1 and C_0 respectively.

TABLE 1

Physical and electromagnetic properties of the considered materials

	Density (ρ) (kg/m^3)	Electric conductivity (σ) (S/m)	Relative magnetic permeability (μ_r)
Aluminum	2700	$3{\cdot}902 \times 10^7$	1
Copper	8960	$6{\cdot}293 \times 10^7$	1
Nickel	8880	$1{\cdot}636 \times 10^7$	200

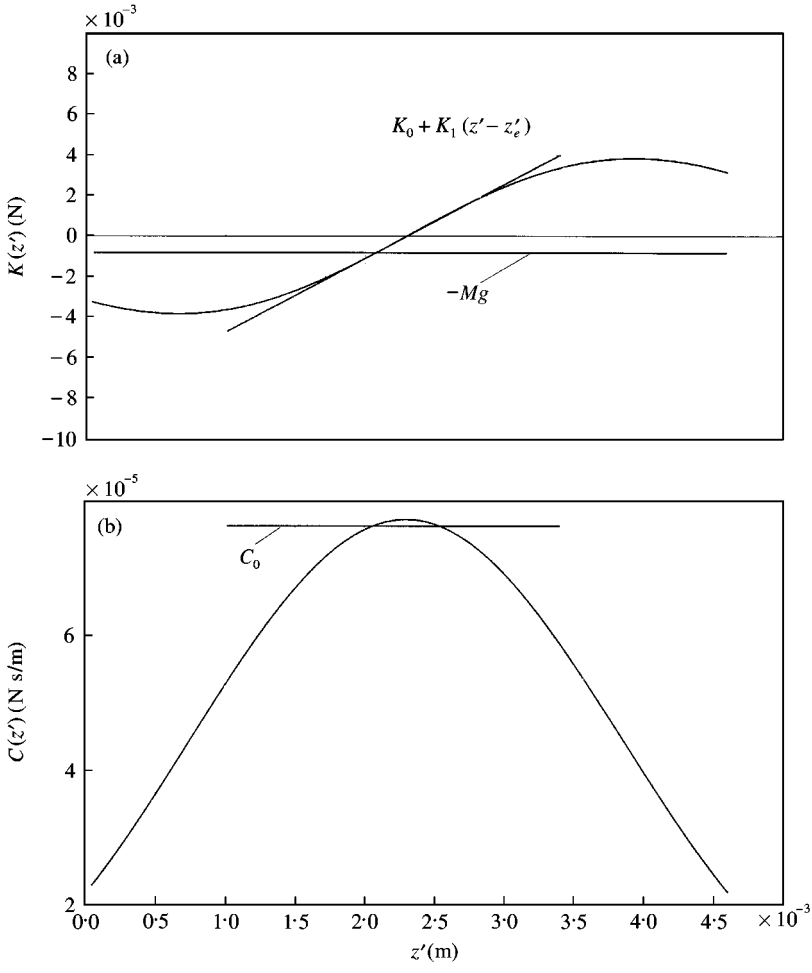

Figure 2. Typical plot for (a) $K(z')$, (b) $C(z')$ versus z' for an aluminum specimen. $I_1 = I_2 = 600$ A, $f = 300$ kHz, $R = 2{\cdot}0$ mm, $b'_1 = b'_2 = 6{\cdot}0$ mm, $h'_2 - h'_1 = 4{\cdot}6$ mm.

Regarding the numerical computation of the infinite series in equations (38) and (39), truncation at six terms for the series in n, and at 18 terms for the series in p and s are sufficient to obtain correct results to four significant figures within an upper error bound of 0·1%. The Mathematica 3·0 [15] package was used to integrate numerically6 the equation of motion (37).

Numerical simulations were performed for a levitation system composed of two current loops having the radii $b'_1 = b'_2 = 6{\cdot}0$ mm and the position co-ordinates h'_1 and h'_2, respectively, with respect to the fixed reference frame. Calculations were done for spherical specimens of aluminum and copper. The initial position was $\frac{1}{4}(h'_1 + h'_2)$. Every loop carried an electric current ± 600 A r.m.s. which is positive for the lower loop and negative for the upper loop ($I_1 = -I_2 = 600$ A). The frequency of the current was $f = 300$ kHz. Ten equally spaced values for the radius R in the range 0·5–2·0 mm and for the distance $h'_2 - h'_1$ in the range 4·6–10·0 mm were considered. Figure 3 shows the results for the integration of equation (37) for three different geometric parameter sets. The values of the considered parameters were $R = 0{\cdot}5$ mm, $h'_2 - h'_1 = 4{\cdot}6$ mm, $R = 1{\cdot}25$ mm, $h'_2 - h'_1 = 4{\cdot}6$ mm, and

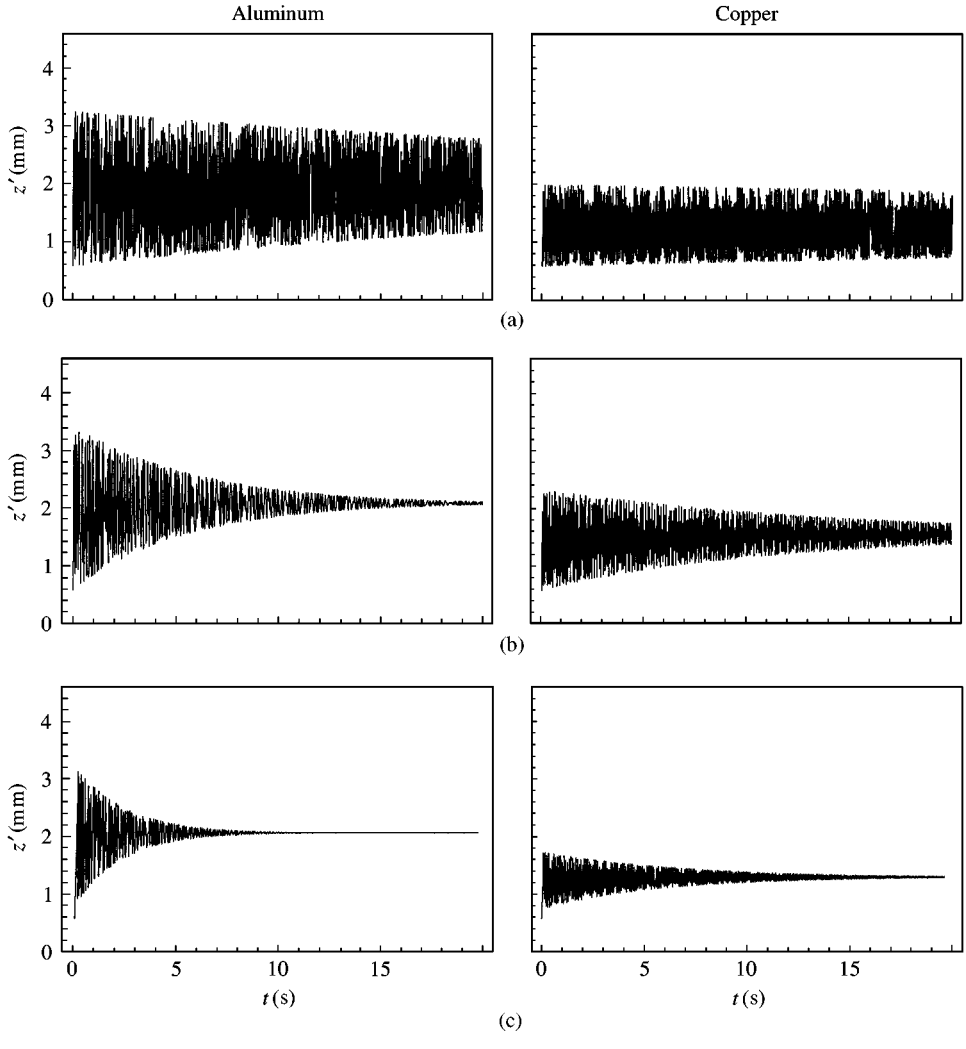

Figure 3. Numerical simulations of the non-linear equation of motion for (a) $R = 0{\cdot}5$ mm, $h'_2 - h'_1 = 4{\cdot}6$ mm, (b) $R = 1{\cdot}25$ mm, $h'_2 - h'_1 = 4{\cdot}6$ mm, (c) $R = 2{\cdot}0$ mm, $h'_2 - h'_2 = 4{\cdot}6$ mm. $I_1 = -I_2 = 600$ A, $f = 300$ kHz, $b'_1 = b'_2 = 6{\cdot}90$ mm.

$R = 2{\cdot}0$ mm, $h'_2 - h'_1 = 4{\cdot}6$ mm and the results shown in Figures 3(a), 3(b) and 3(c) respectively.

The linearized model developed in section 2.4 was used to estimate the damping and natural frequency. After identifying the coefficients of the linearized equation of motion (46), the damping factor and natural frequency were computed by using equations (47) and (48) respectively. Figures 4(a) and 4(b) show the contour plots for the damping factor ξ for aluminum and copper specimens respectively. The dimensionless quantities $(h'_2 - h'_1)/b'_1$ and R/δ, where $\delta = 1/\pi f \mu_i \sigma$ is the skin depth, were considered. Similarly, Figures 5(a) and 5(b) show the contour plots for the natural frequency $f_n = \omega_n/2\pi$. The natural frequency was also computed by applying Holmes linearized theory [8] in Tables 2 and 3. These tables list the values of the natural frequency for aluminum and copper, respectively, obtained from equation (48) (denoted by f_n) and equation (24) (p. 3104 in Holmes paper (denoted by f_{nH}).

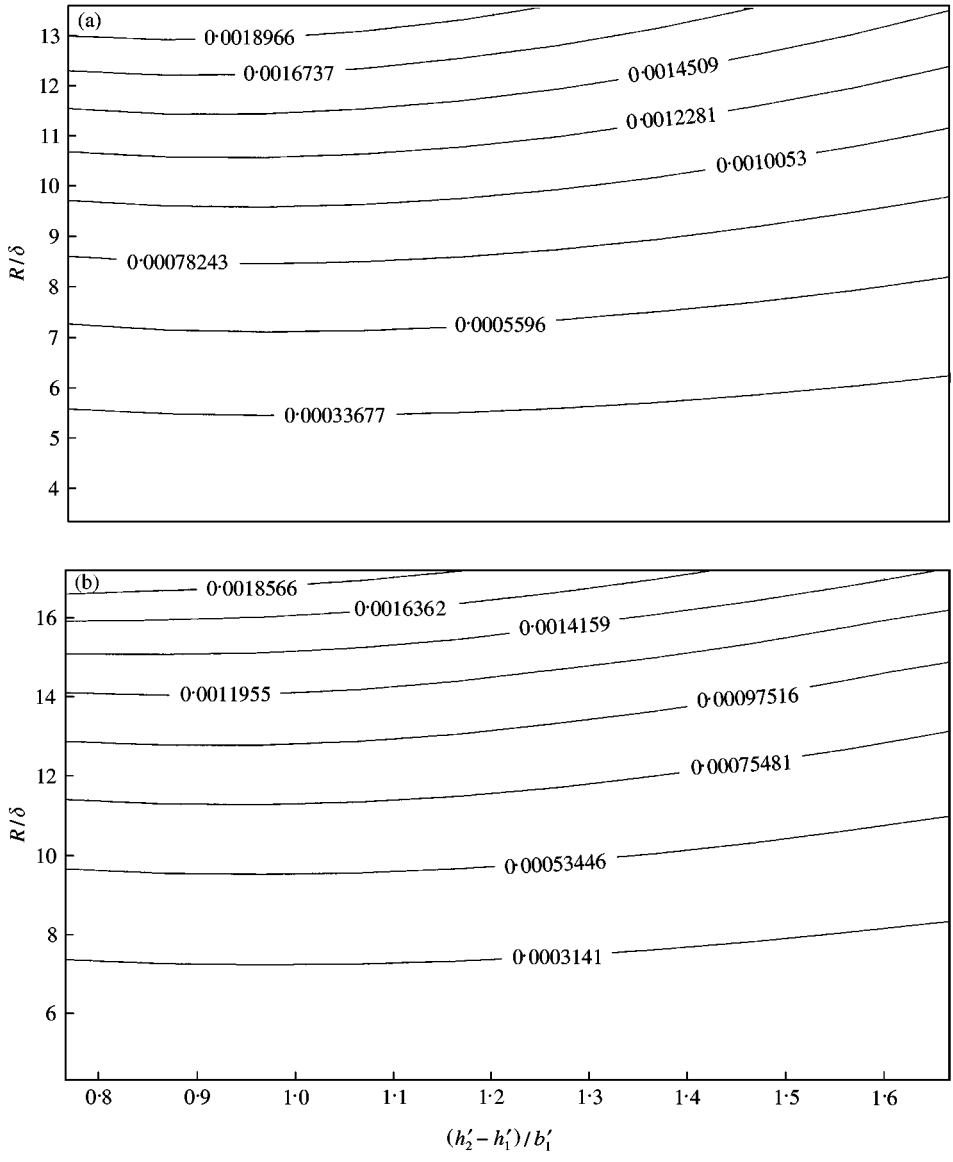

Figure 4. Contour plot for the damping factor ξ calculated for (a) aluminum specimens, (b) copper specimens. $I_1 = I_2 = 60{\cdot}0$ A, $f = 300$ kHz, $b'_1 = b'_2 = 6{\cdot}0$ mm.

One can observe a very good agreement between the results obtained in both ways. This outcome helps validate our mathematical model.

The approach proposed in this work may be a start point for the coil design. The expression of the levitation force due to the motion of specimens developed in section 2.1 can be used to estimate the damping in the levitation system. Linearizing the equation of motion about the equilibrium position of the specimens, one can calculate the damping factor and the natural frequency. Hence, regions of stable and desired damped levitation along the vertical axis of the coil can be predicted, a fact that helps design good levitation coils.

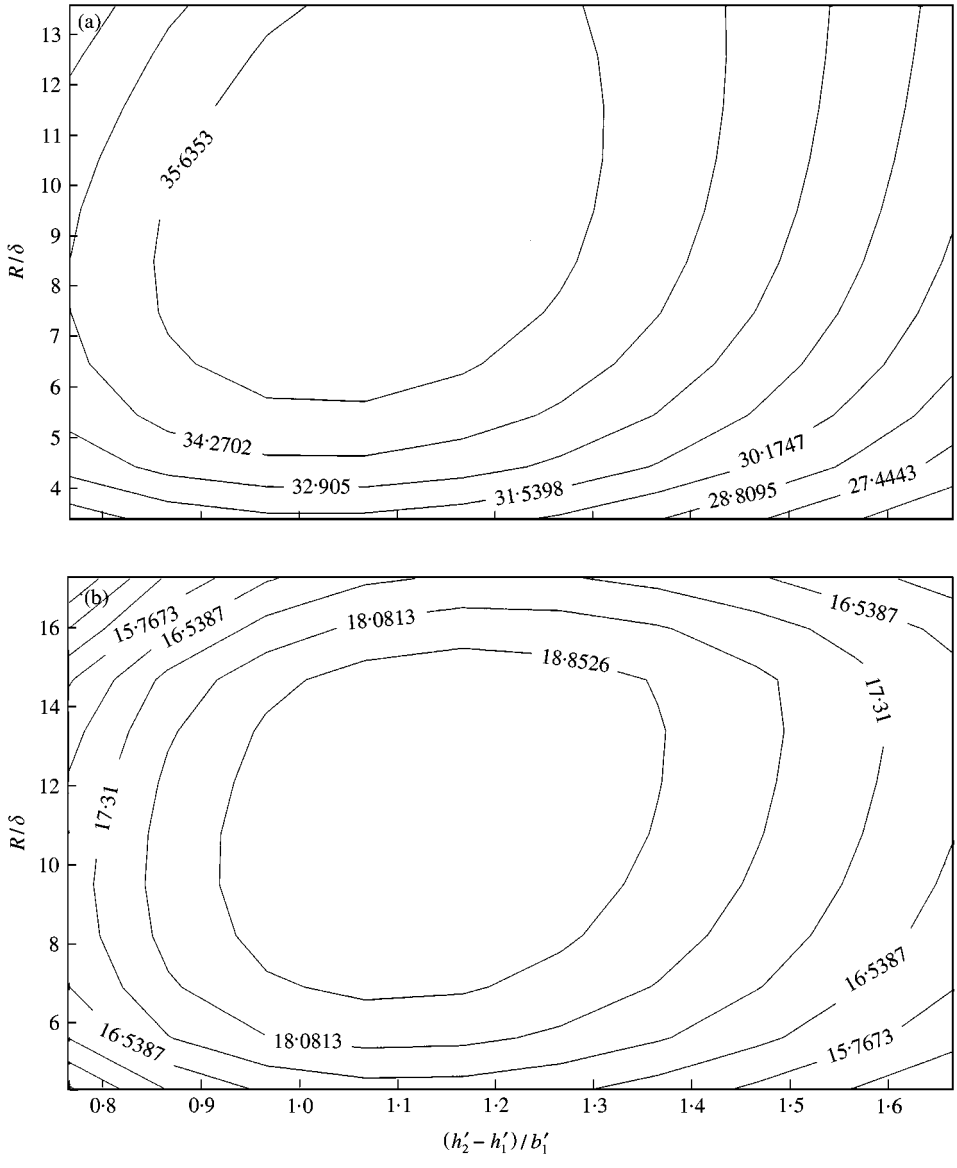

Figure 5. Contour plot for the natural frequency f_n calculated for (a) aluminum specimens, (b) copper specimens. $I_1 = I_2 = 600$ A $f = 300$ kHz, $b'_1 = b'_2 = 6{\cdot}0$ mm.

4. CONCLUSIONS

The vertical motion of a spherical metal levitated by two parallel loops carrying electric currents in opposed direction was considered. The mathematical model of the motion was developed and simulations were performed. The behavior of aluminum and copper specimens was studied for various parameter sets of the levitation system. The equation of motion was linearized about the equilibrium position and the damping factor and natural frequency were estimated. The natural frequency was also computed and favourably compared with other reported works.

TABLE 2

The natural frequency computed by applying our approach (f_n) and Holmes theory (f_{nH}) for aluminum specimens

	$h'_2 - h'_1 = 4{\cdot}6$ mm		$h'_2 - h'_1 = 5{\cdot}8$ mm	
R (mm)	f_n (Hz)	f_{nH} (Hz)	f_n (Hz)	f_{nH} (Hz)
0·50	29·47	29·36	31·26	31·20
0·95	33·98	33·90	36·16	36·12
1·25	34·27	34·07	36·74	36·70
1·70	33·26	33·04	36·23	36·11
2·00	31·94	31·69	35·34	35·22
	$h'_2 - h'_1 = 7{\cdot}0$ mm		$h'_2 - h'_1 = 10{\cdot}0$ mm	
0·50	30·81	30·76	24·71	24·71
0·95	35·81	35·78	28·97	28·98
1·25	36·62	36·59	29·97	29·98
1·70	36·63	36·55	30·73	30·75
2·00	36·18	36·11	31·02	31·02

TABLE 3

The natural frequency computed by applying our approach (f_n) and Holmes theory (f_{nH}) for copper specimens

	$h'_2 - h'_1 = 4{\cdot}6$ mm		$h'_2 - h'_1 = 5{\cdot}8$ mm	
R (mm)	f_n (Hz)	f_{nH} (Hz)	f_n (Hz)	f_{nH} (Hz)
0·50	14·10	11·85	16·66	15·52
0·95	16·86	15·40	19·10	18·31
1·25	16·84	15·35	19·25	18·49
1·70	15·68	13·84	18·62	17·79
2·00	12·68	9·52	16·44	15·25
	$h'_2 - h'_1 = 7{\cdot}0$ mm		$h'_2 - h'_1 = 10{\cdot}0$ mm	
0·50	16·99	16·23	14·32	14·21
0·95	19·33	18·81	16·15	16·06
1·25	19·62	19·13	16·56	16·50
1·70	19·35	18·87	16·78	16·76
2·00	17·42	16·76	15·39	15·35

ACKNOWLEDGMENTS

The authors gratefully acknowledge the financial support received from NASA's Office of Life and Microgravity Sciences and Applications under Cooperative Agreement No. NCC8-128. The authros also acknowledge Drs Dan B. Marghitu and Deming Wang for helpful discussions.

REFERENCES

1. O. MUCK 1923 *German Patent* 422004.
2. W. BRISLEY and B. S. THORNTON 1963 *British Journal of Applied Physics* **14**, 682–686. Electromagnetic levitation calculations for axially symmetric systems.
3. P. R. RONY 1964 *Transactions of Vacuum Metallurgy Conference*, 55–135. The electromagnetic levitation of metals.
4. G. LOHÖFER 1989 *SIAM of Applied Mathematics* **49**, 567–581. Theory of an electromagnetically levitated metal sphere I: absorbed power.
5. D. L. CUMMINGS and D. A. BLACKBURN 1991 *Journal of Fluid Mechanics* **224**, 395–416. Oscillations of magnetically levitated aspherical droplets.
6. A. J. MESTEL 1982 *Journal of Fluid Mechanics* **117**, 27–43. Magnetic levitation of liquid metals.
7. E. S. BOCIAN and F. J. YOUNG 1971 *Journal of Electrochemical Society*: *Solid State Science* **18**, 2021–2026. Some stability considerations in levitation melting.
8. L. M. HOLMES 1978 *Journal of Applied Physics* **49**, 3102–3019. Stability of magnetic levitation.
9. W. R. SMYTHE 1989 *Static and Dynamic Electricity*. New York: Hemisphere Publishing Corporation.
10. H. H. WOODSON and J. R. MELCHER 1968 *Electromechanical Dynamics*. New York: John Wiley & Sons.
11. B. Q. LI 1994 *International Journal of Engineering Science* **32**, 45–67. The fluid flow aspects of electromagnetic levitation processes.
12. W. T. THOMSON 1981 *Theory of Vibration with Applications*, second edition. Prentice-Hall, Inc. Englewood Cliffs, NJ.
13. D. F. MINER and J. B. SEASTONE 1955 *Handbook of Engineering Materials.* New York: John Wiley & Sons, Inc.
14. R. B. ROSS 1980 *Metallic Materials Specification Handbook*. London: E & F. N. Spon Ltd.
15. *Mathematica* 3.0, Wolfram Research, Inc.